

RESEARCH

Open Access



Investigation and evaluation methods of shallow geothermal energy considering the influences of fracture water flow

Fengqiang Deng¹, Peng Pei^{1*} , Yonglin Ren², Tingting Luo¹ and Yixia Chen¹

*Correspondence:
ppei@gzu.edu.cn

¹ College of Mines, Guizhou University, North Wing Rm 426, Huaxi, Guiyang 550025, Guizhou, China

² Guizhou Lvnengxing New Energy Development Co., Ltd., Guiyang 550001, China

Abstract

The energy replenishment and heat convection induced by fracture water flowing through the rock mass impact the shallow geothermal energy occurrence, transfer and storage mechanisms in it. In this article, a suitability evaluation and categorization system is proposed by including judgement indexes that are more closely aligned with the actual hydrogeological conditions in fracture developed regions; an assessment approach of regional shallow geothermal energy is proposed by coupling the influences of fracture water into the calculation methods of geothermal capacity, thermal balance and heat transfer rate. Finally, by taking two typical fracture aperture distributions as examples, the impacts of fracture water on the investigation and evaluation of shallow geothermal energy are quantitatively analyzed. Although the fracture apertures only share 1.68% and 0.98% of the total length of a borehole, respectively, in the two examples, the fracture water convection contributes up to 11.01% and 6.81% of the total heat transfer rate; and the energy replenishment potential brought by the fracture water is equivalent to the total heat extraction of 262 boreholes. A single wide aperture fracture can dominate the aforementioned impacts. The research results can support more accurate evaluation and efficient recovery of shallow geothermal energy in fracture developed regions.

Keywords: Shallow geothermal, Fractured rock mass, Fracture water, Investigation and evaluation

Introduction

Shallow geothermal energy, which is recovered and utilized by ground source heat pumps (GSHPs), is a type of promising, green and efficient energy (Mao et al. 2015; Zhao et al. 2021; Cui et al. 2018) and its promotion is one of the key approaches in reducing building energy consumption and mitigating greenhouse gas emissions (Lan et al. 2014). The most widely used GSHP is the vertical close-loop system, which exchanges heat with the ground via borehole heat exchangers (BHEs).

Accurate investigation and evaluation is the prerequisite of sustainable utilization and management of shallow geothermal energy. There are national, local and industry standards (DB37/T 4308-2021 2021) and specifications (DZ/T 225-2009 2009) about

the investigation and evaluation of shallow geothermal energy that provide calculation and assessment methods based on general geological and hydrogeological conditions. However, some special conditions are not included in these standards and specifications, such as the karstic environment where fractures and fissures are very developed in the carbonate rock mass where the BHEs are placed. Due to the heat convection and (Mu et al. 2022; Zou et al. 2021) high heat capacity (Zou et al. 2022; Zhou 2020a) brought by the fracture water flow, the heat storage and heat exchange mechanisms are different from that in other regions where the Quaternary layer is thick and groundwater is in pores rather than fractures.

Many previous studies focused on the effect of groundwater on the energy transfer mechanism during shallow geothermal recovery. Abdallah et al. (1995) and Ogino et al. (1999) confirmed the important role of convection in the heat exchange between fracture water and formations, but did not further explore the effect of fracture water characteristics on heat transfer rate of BHE. Xiao et al. (2021) conducted a numerical simulation research to the infiltration and heat transfer in rock mass with single fracture in a geothermal reservoir, and concluded the influence of rate and temperature of injected fluid on the temperature field of rock mass. However, further research in the heat transfer effects of morphological features such as the fracture trace length and aperture is missing. Sun et al. (2021) performed a coupling simulation of groundwater infiltration and heat transfer of ground heat exchanger, extended the two-dimensional fracture network to a three-dimensional borehole group system, and concluded the variation regularity of ground temperature field and heat transfer rate of BHE under different groundwater seepage velocities. Shaik et al. (2011) used a two-dimensional model to simulate the heat extraction process of the geothermal system, and proved that the connectivity of fractures and water flow velocity has a vital influence on the heat extraction efficiency, but only the influence of individual factors such as groundwater velocity and connectivity of fracture on the heat transfer rate were studied. In addition, Aliyu et al. (2017) and Mohais et al. (2011) examined the effect of fracture aperture, injected fluid temperature and formation permeability on the heat transfer process during reservoir development, but research in applications under specific geological conditions and subsequent quantitative analysis to the impact of different geological conditions on heat transfer is not adequate. Considering the heterogenetic strata and corresponding geothermal gradient, Fang et al. (2021) carried out a heat transfer analysis of middle and deep BHEs, which further improved the calculation accuracy.

The aforementioned researches have advanced the understanding of impact of hydrogeological conditions on the heat transfer mechanism between BHE and the ground. However, most researches in vertical closed-loop GSHP applications are based on the quaternary geological conditions and focus on the effects of pore water. While researches focusing on the impacts of fracture water are about the development of deep geothermal reservoirs. Accurate quantitative analysis, especially the influences of fracture water flow to the heat transfer and storage mechanism during shallow geothermal energy evaluation and development is still inadequate, hence the current investigation and evaluation methods of shallow geothermal energy are not well applicable to the karstic environment and other regions where the ground is mainly fractured rock mass.

In this study, the influences of fracture water flow on mechanisms heat transfer, heat storage, energy replenishment and thermal balance are discussed; a suitability evaluation and categorization system is proposed by including judgement indexes that are more closely aligned with the actual hydrogeological conditions in fracture developed regions; an assessment approach of regional shallow geothermal energy is proposed by revising the calculation methods of geothermal capacity, thermal balance and heat transfer rate. Compared with current standards and codes, the proposed indexes and assessment approach emphasis the influences of fracture water flow, and provide more practical and accurate evaluation and efficient recovery of shallow geothermal energy in fracture developed regions.

Methodology

The “Survey of Regional Shallow Geothermal Energy” in the Chinese national standard “*Specification of Shallow Geothermal Energy Investigation and Evaluation* (DZ/T 225-2009 2009) specifies detailed methods in geological survey, suitability categorization, sampling and test, pumping and injection tests, and assessment of regional shallow geothermal energy in terms of geothermal capacity, heat transfer rate of BHE and evaluation of thermal balance. The karstic environment is featured with very thin Quaternary layer (usually less than 10 m), carbonate rock of high heat conductivity, developed water storage and conduit spaces, heterogeneity, and strong hydrological circulation with seasonal fluctuation, which are significantly different from that in the current standards and codes. The fracture water is not Darcy flow, and brings in stronger energy replenishment and heat convection than the pore water. Water saturation further improves the thermophysical properties of ground formation. In this study, based on the unique hydrogeological conditions of karstic ground characteristics, the approach of investigation and evaluation of shallow geothermal energy is revised from the aspects of suitability categorization and the calculation methods of geothermal capacity, heat transfer rate of BHE and thermal balance. The methodology is shown in Fig. 1.

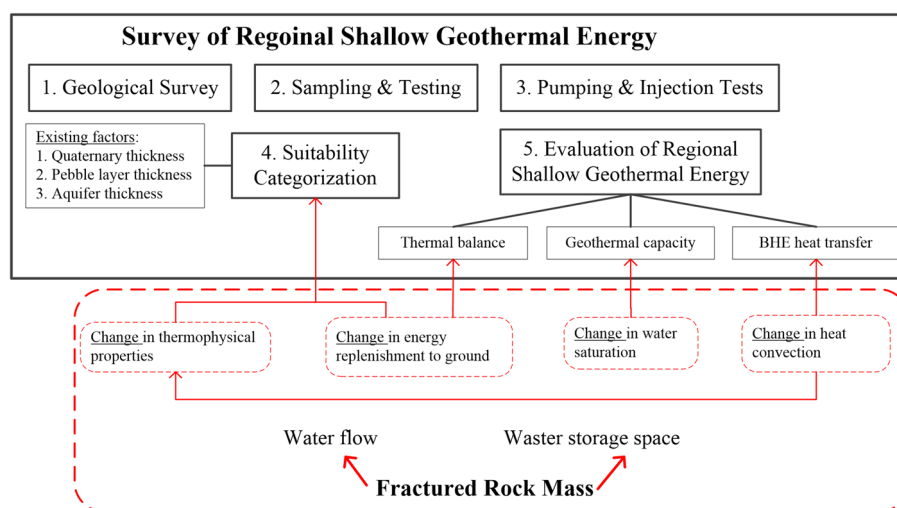


Fig. 1 Methodology

From Fig. 1, it is known that long-term dynamic hydrogeological record is the foundation of the investigation and evaluation work. Ground flow direction is usually determined by water-head triangle method that involves three monitoring wells measuring water tables (Luo et al. 2016). The flow direction is determined by drawing the perpendicular lines to the water table contour map. The velocity of the groundwater flow is commonly determined by tracer tests in borehole field using fluorine or salt (Luo et al. 2016). By measuring the distance along the flow direction and the known time, the velocity of the groundwater flow can be calculated. These methods are mature and easy to operate following standard codes.

In some fracture developed regions, especially the karstic environment, there are some barriers to the application of above methods. First, due to the complicated hydrogeological conditions in the karstic environment, the test wells may not be placed in the same hydraulic system, resulting failure of the tests. Besides, the groundwater circulation at shallow depth is charged by precipitation, showing a strong seasonal fluctuation (Zou et al. 2021). Therefore, long-term and dynamic monitoring of water table and flow rate is necessary, which can be costly, laborious and time consuming by using water-head triangle method and tracer tests. New investigation method based on particle image velocimetry (PIV) technology has potential applicability in dynamic monitoring of fracture water filed. This method captures particle movement in groundwater by high-speed imagination in the borehole, and then the groundwater flow rate and direction can be analyzed by computer visualization of the particle movement (Snow 1969).

Suitability evaluation and categorization

Influence factors

The suitability categorization methods of shallow geothermal development by vertical closed-loop GSHP in current standards, such as the local standard of Shandong Province, China *Specification for investigation and evaluation of regional shallow geothermal energy* (DB37/T 4308-2021 2021) and national standard of China *Specification for shallow geothermal energy investigation and evaluation* (DZ/T 225-2009 2009), are based on Quaternary geological conditions rather than rock fracture developed regions, e.g., karstic environment. In engineering practice, the suitability categorization of shallow geothermal development depends on various factors (Lu 2020), and should be evaluated based on the local hydrogeological conditions.

Judgement factors in the current standards include Quaternary thickness, pebble layer thickness and aquifer thickness (DZ/T 225-2009 2009). From these judgement factors, most areas in the karstic environment would be categorized as *unsuitable*, since the Quaternary layer is very thin and pebble layers are rare. Besides, the heat convection and energy flow brought by fracture water is not sufficiently considered in the calculation of thermal balance and geothermal capacity.

In the karstic environment, the ground energy storage and exchange system (Liu et al. 2018) includes the rock matrix, fracture water, porewater and borehole group. Therefore, the proposed major judgement indexes include thermophysical properties of the rock mass, aquifer properties and energy flow carried by fracture flow. These indexes are considered based on their influences on the geothermal capacity and balance of the energy storage rock mass.

The specific heat capacity, thermal conductivity and thermal expansion coefficient of rock mass are influenced by water content and flow rate in the formation. Since the water source in shallow fractures is mainly from atmospheric precipitation, the thermophysical properties change with seasonal groundwater fluctuation. In general, the convection brought by the fracture flow would enhance energy transfer between BHE and rock mass (Zou et al. 2021). More importantly, the water flow in fracture networks usually is more abundant than pore water flow (Mingzhang et al. 2015), and hence it is expected to have a stronger potential to replenish energy to the rock mass, mitigating the risk of thermal imbalance. Therefore, the in situ thermal response tests, rather than laboratory test, are suggested to conduct at different seasons to obtain more accurate overall thermophysical properties.

The considered aquifer properties include aquifer thickness, flow rate and permeability. Pumping and injection tests are suggested during the regional and site investigation works to understand these parameters to calculate energy flow through the rock mass.

Energy flow carried by fracture water

The fracture flow has a potential to mitigate the thermal imbalance and enhance the thermal renewability of rock mass. Therefore, calculation of the energy flow carried by fracture water is an important prerequisite in evaluation and categorization of site suitability.

The total water flow rate in multiple fractures in the rock mass is calculated by adding that of each fracture at the boundary of control volume that water flows in. The water flow in the fracture plane is decomposed to two components which are parallel to and perpendicular to the trace length, respectively (Fig. 2). In the direction vertical to the trace length, the flow rate per trace length is described by Hoek and Bary (Snow 1969):

$$q_{fr} = \frac{e_i^3 g}{12\nu} J, \quad (1)$$

where q_{fr} (m^2/s) is the flow rate per trace length; e_i (m) is the fracture aperture; ν (m^2/s) is the kinetic viscosity of water; g (m/s^2) is the gravity; and J (m/m) is the hydraulic head loss gradient in the flow direction, which is time dependent.

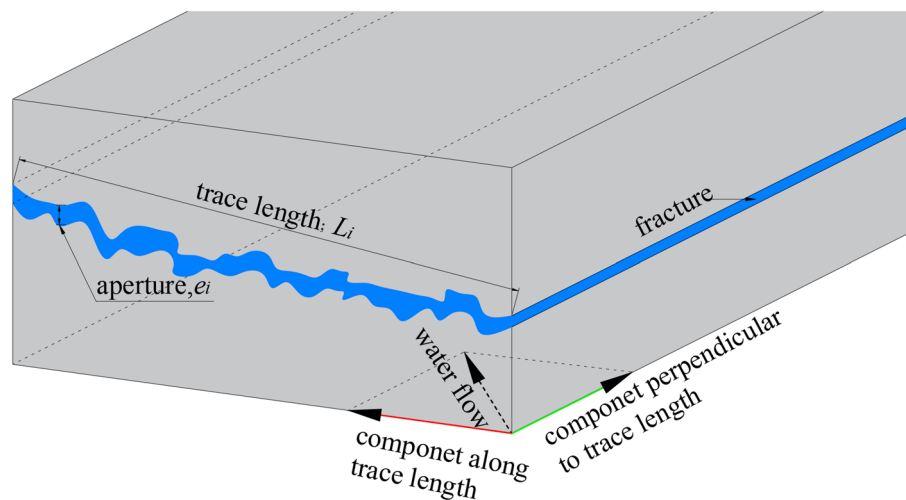


Fig. 2 Fracture dimensions and decomposition of flow direction

The e_i (m) is not constant so the flow rate in the fracture needs to be calculated based on the average aperture in a fracture, \bar{e}_i (m). Therefore, average water flow rate \dot{V}_{fr_i} (m³/s) in a single fracture is given by Eq. (2):

$$\dot{V}_{fr_i} = \bar{e}_i^3 L_i \frac{g}{12\nu} J, \quad (2)$$

where L_i (m) is the trace length of fracture i .

From Eq. (2), the total volumetric water flow rate of all fractures, \dot{V}_{fr} (m³/s), is given by Eq. (3):

$$\dot{V}_{fr} = \sum_{i=1}^n \bar{e}_i^3 L_i \frac{g}{12\nu} J. \quad (3)$$

Since \dot{V}_{fr} (m³/s) is time dependent, the energy flow carried by fracture water is not a constant. The rate of energy flow carried by fracture water, ΔQ_{fr} (W), is given by Eq. (4):

$$\Delta Q_{fr} = \dot{V}_{fr} \rho_{fr} C_{fr} \Delta t_{fr}, \quad (4)$$

where ρ_{fr} (kg/m³) is the water density; C_{fr} [kJ/(kg °C)] is the specific heat capacity of fracture water; and Δt_{fr} (°C) is the available temperature difference between fracture flow and rock mass.

From the above equations, it is shown that the energy flow carried by the fracture water is determined by \bar{e}_i , L_i and Δt_{fr} . Therefore, it is suggested that the fracture water temperature, ground temperature, distribution characteristics of fracture trace length and apertures of rock mass at the engineering site should be counted and investigated. In practice, the fracture development characteristics can be obtained by survey of similar outcrops, the core observation, casting thin slice and imaging logging analysis data. Survey of similar outcrops is the most cost-effective approach in shallow geothermal evaluation. The fractures volume then can be estimated based on the statistic distribution of apertures, lengths and densities.

Adjustment of judgement indexes

The judgement indexes for suitability categorization of shallow geothermal development by vertical closed-loop GSHP in fracture developed regions are proposed in Table 1. The proposed system adopts the thermophysical properties of energy storage rock mass, aquifer properties and energy flow carried fracture water as basic indexes. ΔT (°C) in the table means the temperature difference between fracture flow and the rock matrix. Taking Guizhou Province in south China, a typical karstic landscape (Cheng et al. 2018) as an example, three temperature ranges of $\Delta T < 3$ °C, 3–7 °C, and > 7 °C are adopted.

Assessment of regional shallow geothermal energy

The intensity of shallow geothermal recovery is restricted by the geothermal capacity and renewable period. Assessment of regional shallow geothermal energy shall be conducted to ensure sustainable development and utilization. In this section, equations in the thermal reservoir method given by current standards (DB37/T 4308-2021 2021) are revised to

Table 1 Proposed assessment criteria for suitability categorization of shallow geothermal development by vertical closed-loop GSHP in fracture developed regions (depth < 200 m)

Categorization	Thermophysical properties of energy storage rock mass		Aquifer properties		Energy flow in fracture water		Note
	Overall heat capacity, C_r , kJ/(kg °C)	Overall heat conductivity, λ_r , W/m K	Thickness, H , m	Volumetric water flow rate, q_{max} , 10L/s	Water flow velocity, u , m/s	Departure from rock temperature, ΔT	
Optimum	> 1 (DZ/T 225-2009 2009)	> 1.5 (DZ/T 225-2009 2009)	> 30 (DB37/T 4308-2021 2021; DZ/T 225-2009 2009)	> 10 (very abundant)	> 1000 (Jiang et al. 2018)	> 10 (Cheng et al. 2018)	Meeting all 6 requirements
Suitable	0.5–1 (DZ/T 225-2009 2009)	0.9–1.5 (DZ/T 225-2009 2009)	10–30 (DB37/T 4308-2021 2021; DZ/T 225-2009 2009)	1–10 (abundant)	400–1000 (Jiang et al. 2018)	5–10 (Cheng et al. 2018)	Except optimum and unsuitable indexes
Unsuitable	< 0.5 kJ (DZ/T 225-2009 2009)	< 0.9 (DZ/T 225-2009 2009)	< 10 (DB37/T 4308-2021 2021; DZ/T 225-2009 2009)	0.1–1 (unabundant)	< 400 (Jiang et al. 2018)	< 5 (Cheng et al. 2018)	Meeting at least 4 requirements

better reflect the influences of fracture water on heat storage and transfer mechanisms in rock mass.

Geothermal capacity

The calculation equations of geothermal capacity in current national standard (DB37/T 4308-2021 2021) are revised based on vertical zoning of karstic ground. Along the depth, the formation can be divided into the unsaturated epikarst zone (usually 2–10 m), saturation karst zone (usually to the depth of 100 m), and deep stratum (Mingzhang et al. 2015). Therefore, the energy storage body is divided into 3 hydrogeological zones (Fig. 3).

The original thermal capacity of Zone i , Φ_{Li} (kJ/°C), is calculated by Eq. (5); the original thermal capacity includes thermal capacity in rock matrix, Φ_r (kJ/°C), calculated by Eq. (6), the thermal capacity in pore water, Φ_w (kJ/°C), calculated by Eq. (7); the thermal capacity in fracture water, Φ_{fr} (kJ/°C), calculated by Eq. (8); and the thermal capacity in air in rock pores, Φ_a (kJ/°C), calculated by Eq. (9):

$$\Phi_{Li} = \Phi_r + \Phi_w + \Phi_q + \Phi_{fr}, \quad (5)$$

$$\Phi_r = V \rho_r C_r (1 - \phi - \gamma), \quad (6)$$

$$\Phi_w = V (\omega - \gamma) \rho_w C_w, \quad (7)$$

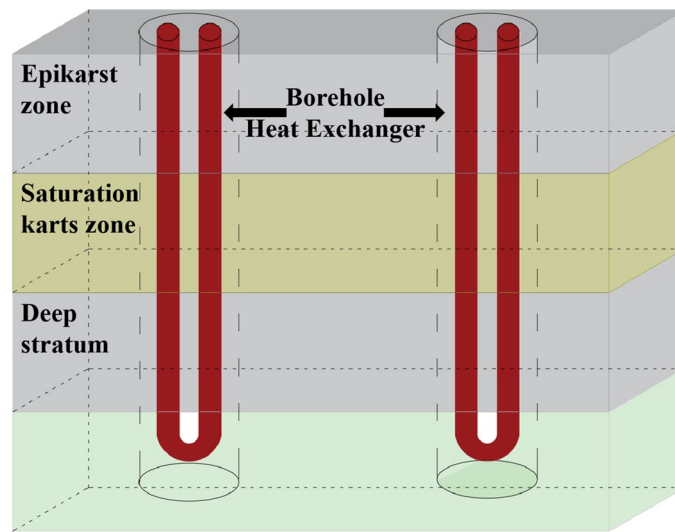


Fig. 3 Hydrogeological zoning of energy storage rock body in karstic environment: epikarst zone (usually 2–10 m), saturation karst zone (usually to the depth of 100 m), and deep stratum

$$\Phi_{fr} = V\gamma\rho_w C_w, \quad (8)$$

$$\Phi_a = V(\varphi + \gamma - \omega)\rho_a C_a, \quad (9)$$

where $V(\text{m}^3)$ is the total volume of energy storage rock mass; $\rho_r(\text{kg}/\text{m}^3)$ is the rock density; $C_r [\text{kJ}/(\text{kg } ^\circ\text{C})]$ is the specific heat of rock; φ is the porosity of rock; γ is the fracture ratio; $\rho_w (\text{kg}/\text{m}^3)$ is the density of water; $C_w [\text{kJ}/(\text{kg } ^\circ\text{C})]$ is the specific heat capacity of water; ω is the saturation ration of water in pores; $\rho_a (\text{kg}/\text{m}^3)$ is the air density; and $C_a [\text{kJ}/(\text{kg } ^\circ\text{C})]$ is the specific heat of air.

The fracture ratio is calculated by Eqs. (10) and (11):

$$\gamma = \frac{V_{fr}}{V}, \quad (10)$$

$$V_{fr} = \sum_{i=1}^n \bar{e}_i L_i d_i, \quad (11)$$

where $V_{fr} (\text{m}^3)$ is the fracture volume; and $d_i (\text{m})$ is the depth of fracture i .

The total thermal capacity of the heat reservoir $\Phi_L (\text{kJ}/^\circ\text{C})$ is the sum of these of all layers by Eq. (12):

$$\Phi_L = \sum_{i=1}^n \Phi_{L_i}. \quad (12)$$

The fracture water has an obvious impact to the thermal capacity of the reservoir. Usually, the fracture ratio γ ranges between 2 and 5%, and reaches up to more than 10% (Yang et al. 2008) in cases when karstic bodies are developed. Therefore, it is suggested that fracture characteristics should be examined and recorded during the site

investigation and resources assessment, including distribution characters of aperture, trace length, fracture depth and water velocity.

Heat transfer rate of BHEs

The total heat transfer rate of a BHE group, Q_h (kW), is the product of a single borehole (DB37/T 4308-2021, 2021; DZ/T 225-2009, 2009), Q_i (W), and the number of boreholes, n , by Eqs. (13) and (14):

$$Q_h = Q_i \times n \times 10^{-3}, \quad (13)$$

$$Q_i = q_i \times l_i, \quad (14)$$

where q_i (W/m) is the heat exchange rate per length of borehole; and l_i (m) is the length of a borehole.

At the intersections between the borehole and water conducting fractures, the heat transfer rate is significantly improved by convection (Zhou 2020b). The total heat transfer rate by convection at all intersections, Q_w (W), is the sum of local heat transfer rate at each intersection, Q_{wi} (W), and can be calculated by Eq. (15) (Yang and Tao 2006):

$$Q_w = \sum_{i=1}^n Q_{wi} = \sum_{i=1}^n h \Delta t_{w-p} S_i = h \Delta t_{w-p} \pi d \sum_{i=1}^n \bar{e}_i, \quad (15)$$

where h [W/(m² k)] is the convective heat transfer coefficient between fracture flow and pipe; Δt_{w-p} (K) is the average temperature difference between fracture flow and BHE; S (m²) is the contact area between fracture flow and pipe; and d (m) is the diameter of the equivalent tube bundle of U-bend loop.

The heat conduction rate between the BHE and rock matrix excluding the fractures, Q_b (W), is given by Eq. (16) (Yang and Tao 2006):

$$Q_b = \frac{2\pi l_i \Delta t_{1-4}}{\frac{1}{\lambda_w} \ln \frac{r_2}{r_1} + \frac{1}{\lambda_2} \ln \frac{r_3}{r_2} + \frac{1}{\lambda_3} \ln \frac{r_4}{r_3}}, \quad (16)$$

where λ_w [W/(m k)] is the conductivity of the wall of buried pipe; λ_2 [W/(m k)] is the conductivity of back fill material in borehole; λ_3 [W/(m k)] is the conductivity of the surrounding formation; Δt_{1-4} (K) is the average temperature different between the energy carrier fluid in the pipe and the rock mass; r_1 (m) is the radius of equivalent tube bundle of buried pipe; r_2 (m) is the outer radius of equivalent tube bundle of buried pipe; r_3 (m) is the radius of the borehole; and r_4 (m) is the thermal effect radius around the borehole.

Therefore, the total heat transfer rate of a single BHE penetrating formation matrix and fractures is given by the sum of the conduction and convection:

$$Q_i = Q_w + Q_b. \quad (17)$$

Since the borehole spacing is much larger than its diameter, a borehole can be considered as a single cylinder, and its convective heat transfer coefficient (Yang and Tao 2006) with the fracture water is given by Eqs. (18, 19, 20):

$$h = Nu \cdot \frac{\lambda_{fr}}{d}, \quad (18)$$

$$Nu = 0.3 + \frac{0.62 Re_f^{\frac{1}{2}} Pr^{\frac{1}{3}}}{\left[1 + \left(\frac{0.4}{Pr}\right)^{\frac{2}{3}}\right]^{\frac{1}{4}}} \left[1 + \left(\frac{Re_f}{282000}\right)^{\frac{5}{8}}\right]^{\frac{4}{5}}, \quad (19)$$

$$Re_f = \frac{ud}{\nu}, \quad (20)$$

where Nu is the Nusselt number; λ_{fr} [W/(m·k)] is the conductivity of fracture water; Re_f is the Reynolds number of fracture water; Pr is the Prandtl number; and u (m/s) is the fracture flow velocity.

Thermal balance

In the karstic environment, the fracture water is abundant and the energy it carries is a significant replenishment source to the energy storage rock mass, and is beneficial to the mitigation of thermal imbalance and sustainable development of geothermal energy. This section quantitatively analyzes the energy replenishment ability of the fracture water and the consequent influence on the thermal balance.

Taking the heating condition in the winter as an example, different types of energy flowing through the rock mass are shown in Fig. 4.

According to the method given by the National Standard of China *Specification for shallow geothermal energy investigation and evaluation* (DB37/T 4308-2021, 2021), the energy balance of the rock mass in a certain period is assessed by Eq. (21):

$$\Delta Q_r = Q_{in} - Q_{out}, \quad (21)$$

where ΔQ_r (kJ) is the change of energy in the rock mass; Q_{in} (kJ) is the energy flowing into the rock mass; and Q_{out} (kJ) is the energy flowing out the rock mass.

In a certain assessment period, if ΔQ_r (kJ) approaches to 0, it means the formation keeps in thermal balance status.

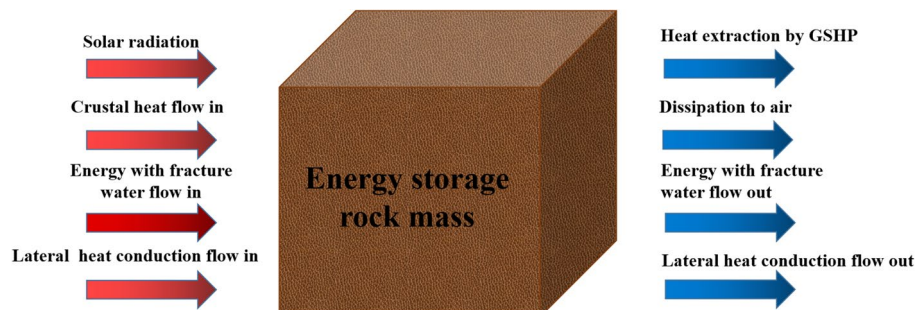


Fig. 4 Energy flow through the storage rock body (heating condition)

The fracture water flow rate is a function of time rather than a constant, so the rate of energy replenishment by fracture water, $\Delta \dot{Q}_{fr_p}$ (kW), which is also a function of time τ , is given by Eq. (22):

$$\Delta \dot{Q}_{fr_p} = \dot{V}_{fr} \rho_{fr} C_{fr} (t_{fr_in} - t_{fr_out}), \quad (22)$$

where t_{fr_in} (°C) is the temperature of fracture water flowing into the rock mass; and t_{fr_out} (°C) is the temperature of fracture water flowing out the rock mass.

The thermal balance equation for an evaluated duration from τ_1 and τ_2 is revised by adding the energy replenishment by fracture water to Eq. (21):

$$\Delta Q_r = Q_{in} - Q_{out} + \int_{\tau_1}^{\tau_2} \Delta \dot{Q}_{fr_p} d\tau. \quad (23)$$

The replenishment energy brought by fracture water can support additional number of BHE, Δn , which is given by Eq. (24):

$$\Delta n = \frac{\Delta Q_{fr_p}}{Q_i}. \quad (24)$$

In current investigation approach, the energy replenishment ability of fracture water is ignored, so as the additional number of heat exchange boreholes it can support given by Eq. (24), and less boreholes are arranged than that the site can actually accommodate, hence reducing the load that the GSHP project can undertake. Therefore, it is clear that understanding the fracture water velocity and distribution characteristics of fractures at the site investigation phase is import to accurately evaluate the thermal balance of the energy storage rock mass and the number of boreholes it can appropriately support.

Case application and discussion

Fracture distribution characteristics

In this section, a quantitative analysis to the influence of fracture water on heat exchange and geothermal capacity in rock mass is performed through typical examples. According to the statistical research on fracture apertures (Deng et al. 1996; Wang 2011; Alexandre et al. 2023), it is assumed that the value of apertures follows the negative exponential distribution. Therefore, two typical fracture networks, Fracture Network I (FN I) and Fracture Network II (FN II), are used as examples:

FN I includes fractures with apertures of 0.5 mm, 1 mm, 1.5 mm, 3 mm, 6 mm, 12 mm whose frequencies are shown in Fig. 5a; and

FN II includes fractures with apertures of 0.5 mm, 1 mm, 1.5 mm, 2 mm, 3 mm, 4 mm whose frequencies are shown in Fig. 5b.

Compared with FN II, there are wide fractures with aperture of 12 mm in FN I.

Assumed parameters used in calculations are assumed in Table 2. According to Wang's (Wang 2011) statistical results of fracture characteristics, the average trace length L_i (m) is assumed as 3 m.

The fracture density in vertical direction is assumed to be 15 according to literatures (Zhou et al. 2017; Wen et al. 2017). The total number of fractures n in the rock mass whose height l (m) is 150 m is given by Eq. (25):

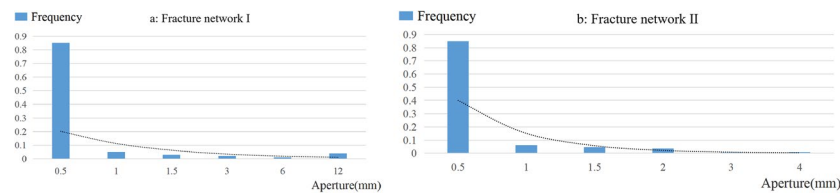


Fig. 5 Examples of statistical distribution of apertures (**a** fracture network I, **b** fracture network II)

Table 2 Assumed parameters used in the case study

Parameter	Value	Parameter	Value
Average trace length L_f (m)	3 (Wang 2011)	Fracture density in vertical direction K	15 (Zhou et al. 2017; Wen et al. 2017)
Viscosity coefficient of groundwater ν (m ² /s)	1.003×10^{-6} (Xu and Yu 2022)	The fracture water head gradient J	0.001 (Huang et al. 2020)
The inner diameter of U-bend loop d (m)	0.026 (Ou 2011)	The borehole diameter (m)	0.15
The borehole depth l_f (m)	150	The average temperature difference between fracture flow and borehole in winter Δt_{w-p} (°C)	10
The fracture water velocity is assumed to be high u (m/s)	3×10^{-4}	The fracture water velocity is assumed to be medium u (m/s)	7×10^{-4}
The fracture water velocity is assumed to be low u (m/s)	1.1×10^{-3}	The specific heat capacity of carbonate rock kJ/(kg °C)	0.58
The porosity of carbonate rock	5%	Saturation of pore waster	3%

$$n = Kl. \quad (25)$$

There are 2250 fractures in each fracture network. The fractures are assumed to follow the distribution in Fig. 5a and b, respectively, and the numbers of fractures of 6 different apertures are calculated (Table 3).

Assuming the viscosity coefficient of groundwater is 1.003×10^{-6} m²/s (Xu and Yu 2022), the fracture water head gradient is 0.001 (Huang et al. 2020) flowing through the rock mass, the total volumetric flow rates are calculated as 0.3961 m³/s in FN I and 0.0056 m³/s in FN II, respectively.

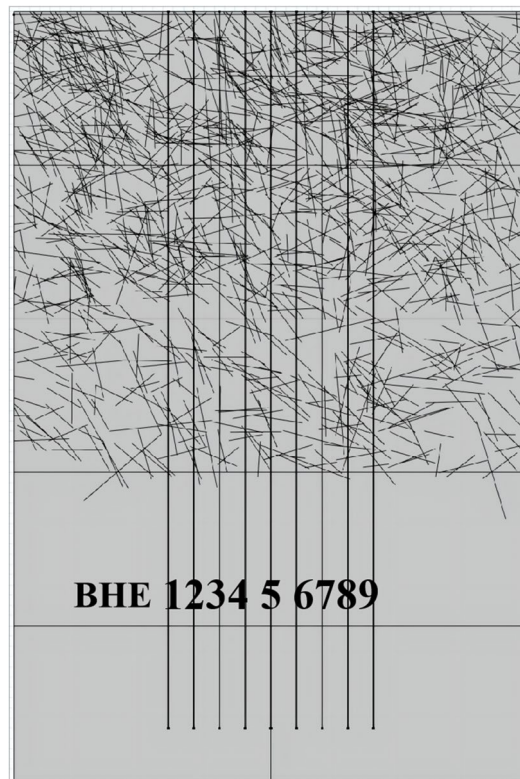
Calculation of heat transfer rate of BHE

The fracture network usually consists of more than one group of fractures. An example is shown in Fig. 6, where the nine boreholes penetrate through the fracture network. The discrete fracture network was generated by the Monte Carlo algorithm with average trace length of 3 m following normal distribution, and average dip of 60° following normal distribution. The groundwater flowing through the fracture network results in convective heat transfer.

Assuming that the inner diameter of U-bend loop is 0.026 m (Ou 2011); the borehole diameter is 0.15 m; the borehole depth is 150 m; and Δt_{w-p} is 10 °C in the winter. The fracture water velocity is assumed to be high (3×10^{-4} m/s), medium (7×10^{-4} m/s) and

Table 3 Calculated volumetric fracture water flow rates in FN I and FN II

FN I						
Aperture, mm	0.5 mm	1 mm	1.5 mm	3 mm	6 mm	12 mm
Frequency, %	85	5	3	2	1	4
Number of fractures	1913	113	68	45	23	90
Trace length, m	3	3	3	3	3	3
Volumetric flow rate, (m ³ /s)	5.84×10^{-4}	2.75×10^{-4}	5.56×10^{-4}	2.97×10^{-3}	1.19×10^{-2}	3.80×10^{-1}
FN II						
Aperture, mm	0.5	1	1.5	2	3	4
Frequency, %	85	6	4.5	3.5	0.6	0.4
Number of fractures	1913	135	101	79	14	9
Trace length, m	3	3	3	3	3	3
Volumetric flow rate, (m ³ /s)	5.84×10^{-4}	3.30×10^{-4}	8.35×10^{-4}	1.54×10^{-3}	8.90×10^{-4}	1.41×10^{-3}

**Fig. 6** An example of typical fracture network

low (1.1×10^{-3} m/s) scenarios, respectively, according to survey data (Jiang et al. 2018). The calculated total heat transfer rate of borehole by convection in FN I and FN II fractures is listed in Table 4.

Assuming that the heat transfer rate per length only by conduction between the borehole and carbonate rock matrix is 40 W/m (Ma and Lv 2007), the total heat transfer rate of fractures in FN I and FN II are calculated by Eqs. (15, 16, 17). The share of convection by fracture water in total heat transfer of single borehole is calculated (Table 4). In

Table 4 Influences of fracture water flow on heat transfer rate of single borehole in FN I and FN II in the case study

FN	FN I			FN II		
Sum of apertures, m	2.520			1.477		
Water velocity, u , (m/s)	3×10^{-4}	7×10^{-4}	1.1×10^{-3}	3×10^{-4}	7×10^{-4}	1.1×10^{-3}
Coefficient of heat convection, h , W/(m ² K)	32.77	49.54	61.92	32.77	49.54	61.92
Total heat transfer rate by convection $Q_{w,r}$, W	388.93	588.05	734.95	227.95	344.67	430.76
Heat transfer rate by convection per length of borehole, $q_{w,r}$, W/m	154.34	233.35	291.65	154.34	233.35	291.65
Heat conduction Q_b , W	5899.2			5940.92		
Total heat transfer rate of a single borehole, W	6329.85	6528.97	6675.87	6127.15	6243.87	6329.96
Share of convection by fracture water in total heat transfer of single borehole	6.14%	9.01%	11.01%	3.72%	5.52%	6.81%

FN I fracture, although the apertures (2.520 m in total) only share 1.68% of the total length of a borehole (150 m), the fracture water contributes 6.14–11.01% of the total heat transfer rate. In FN II fracture, the apertures (1.477 m in total) only share 0.98% of the total length of a borehole, but the fracture water contributes 3.72–6.81% of the total heat transfer rate.

Calculation of thermal capacity and thermal balance of rock mass

The calculation follows Eqs. (5, 6, 7, 8, 9, 10, 11, 12). In most engineering practices, the spacing between boreholes usually is 5 m, so an imaginary energy storage rock mass of 150 m high and 5 m wide is assumed, where the boreholes are placed along the groundwater flow direction as shown in Fig. 7. The fracture ratios γ_I and γ_{II} are calculated as 1.008% and 0.5908%, respectively. Assuming that the specific heat capacity of carbonate rock is 0.58 kJ/(kg °C) (Song et al. 2019); the porosity is 5%; and saturation of pore water is 3%, the thermal capacities of fracture water in FN I and FN II, Φ_{fr-I} and Φ_{fr-II} , are calculated as 2.56% and 1.50% of the total thermal capacity of the rock mass.

Assuming that the temperature change of fracture water flowing through the rock mass is 1 °C, the rate of energy replenishment by fracture water can be calculated by Eqs. (1, 2, 3, 4). The results are $\Delta Q_{fr-p,I}$ in FN I is 1663.78 kW and $\Delta Q_{fr-p,II}$ in FN II is 23.46 kW, respectively.

Borehole placement optimization

The energy replenishment by fracture water calculated in Sect. “Calculation of thermal capacity and thermal balance of rock mass” can be utilized to undertake additional heating load. According to the designing code (Ma and Yao 2009), the specific heating load is 80 W/m² for public buildings, 70 W/m² for residence buildings, and 160 W/m² for indoor stadiums, respectively. If FN I fractures exist in the rock mass, the $\Delta Q_{fr-p,I}$ of 1663.78 kW can support an additional heating area of 20797 m² in public building, 23768 m² in residence building and 10399 m² in indoor stadium. Similarly, the $\Delta Q_{fr-p,II}$ of 23.46 kW in FN II can support an additional heating area of 293 m² in public building, 335 m² in residence building and 147 m² in indoor stadium.

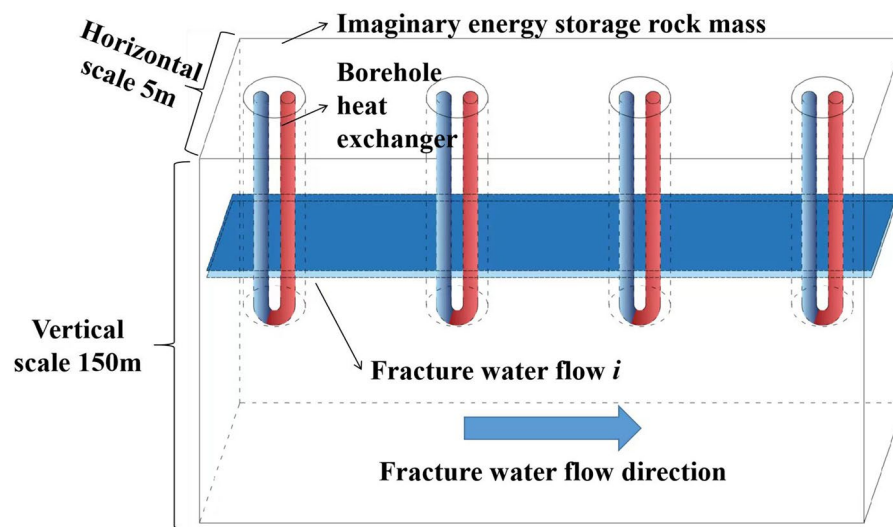


Fig. 7 Proposed borehole placement optimization and fracture water in an imaginary energy storage rock mass

Table 5 Additional heat exchange boreholes undertaken by energy replacement from fracture water in the case study

Water velocity, u , (m/s)	3×10^{-4}	7×10^{-4}	1.1×10^{-3}
Additional boreholes in FN I	262	254	249
Additional boreholes in FN II	3	3	3

According to the calculation results in Sect. “[Calculation of heat transfer rate of BHE](#)”, when the water velocity is high (1.1×10^{-3} m/s) in FN I fractures, the total heat transfer rate of a single borehole is 6.68 kW. Assuming that the boreholes can be lay out along the fracture water flow direction without constraint, the $\Delta Q_{fr,p,I}$ of 1663.78 kW can undertake up to 249 additional boreholes from Eq. (23). The calculation result for FN II is also listed in Table 5.

The above results provide a support for optimization of boreholes placement along the flow direction to make the best use of the energy replenishment by fracture water. It is suggested that fracture water direction should be detected during the investigation phase, and the boreholes should be placed along the flow direction as much as possible.

It is obvious that the wide aperture fractures play a dominating role in energy replenishment. This is because the volumetric flow rate of water is proportional to the cube of aperture, and a wide aperture fracture would dominate the total flow volume in the fracture network (Hudson and Harrison 1997).

Conclusion

A suitability evaluation and categorization system specialized for shallow geothermal recovery in fracture developed regions is proposed by optimizing evaluation parameters in thermophysical properties of rock mass, aquifer properties and fracture water characteristics. The calculation methods of geothermal capacity and thermal balance of rock

mass are proposed based on the hydrogeological conditions aligned with the fracture developed environment. Compared with current standards and codes, the proposed indexes and assessment approach emphasize the influences of fracture water flow. The fracture water has an obvious influence on geothermal capacity, thermal balance and heat transfer rate of BHE. It is suggested that, during the investigation phase, fracture characteristics including aperture, trace length, water velocity and temperature should be obtained to support more accurate evaluation of geothermal capacity and thermal balance.

The energy replenishment carried by fracture water flow should be utilized to reduce thermal imbalance risk and improving system stability. In engineering practice, supplementary systems such as air source heat pumps or boilers are used to keep the balance between heat extraction and discharge to the formation. However, in the case that the fracture water is abundant and has a strong ability to replenish energy to the rock mass, the supplementary system can be reduced or even eliminated, hence decreasing investment and improving economics of the project.

The fractures of wide aperture would dominant the energy flow in the whole fracture network, playing a key role in influencing the energy transfer and replenishment process, so it is suggested that the boreholes should be placed in locations where wide aperture fractures are developed to take advantage of water flow to enhance heat exchange and thermal balance. However, such a placement might increase the difficult and cost in borehole drilling and backfilling.

Since the source of fracture water at shallow depth is the precipitation with strong seasonal fluctuation, hydrogeological data are important in design and optimization of ground heat exchanger, as well as operation strategy of the closed-loop GSHP system. In regional investigation of shallow geothermal resources, dynamic monitoring systems should be established to follow the seasonal fluctuation of velocity, temperature and flow rate of groundwater; and advanced devices which are fast and conveniently characterize the fractures and water flow inside are necessary.

Acknowledgements

The author appreciates the support from the National Natural Science Foundation of China for the research.

Author contributions

FD: data collection, calculation and writing; PP: resourcing, project management and revise; YR: data collection and revise; TL: calculation; YC: calculation.

Funding

This work was supported by the National Natural Science Foundation of China (Grant Number: 52066005).

Availability of data and materials

All data, models, and code used to support the findings of this study are included within the article.

Declarations

Competing interests

The authors declare that they have no known competing financial interests or personal relationships that could have appeared to influence the work reported in this paper.

Received: 28 January 2023 Accepted: 10 August 2023

Published online: 19 August 2023

References

- Abdallah G, Thoraval A, Sfeir A, Piguet JP. Thermal convection of fluid in fractured media. *Int J Rock Mech Min Sci Geomech Abstr.* 1995;32:481–90.
- Alexandre D, Juliana AGL, Walter EM, Denis JS, Vincenzo LB, Francisco HR. Impact of fracture set scales and aperture enlargement due to karstic dissolution on the fluid flow behavior of carbonate reservoirs: a workflow to include sub-seismic fractures in 3D simulation models. *Geoenergy Sci Eng.* 2023;221:211374. <https://doi.org/10.1016/j.geoen.2022.211374>.
- Aliyu MD, Chen HP. Sensitivity analysis of deep geothermal reservoir: effect of reservoir parameters on production temperature. *Energy.* 2017;129:101–13.
- Cheng Q, Wang P, Tan X. Temporal and spatial variation characteristics of surface temperature in Guizhou province from 1961 to 2013. *South-to-North Water Transf Water Conserv Sci Technol.* 2018;16(02):122–31.
- Cui Y, Zhu J, Twaha S. A comprehensive review on 2D and 3D models of vertical ground heat exchangers. *Renew Sustain Energy Rev.* 2018;94:84–114.
- DB37/T 4308-2021 Specification for investigation and evaluation of regional shallow geothermal energy. 2021.
- Deng R, Zhang Z, Huang R, Wang S. Study on the characteristics of rock mass structure in the dam area of Jinping I Hydropower Station. *Geol Hazards Environ Prot.* 1996(01):35–40+53.
- DZ/T 225-2009. Specification for shallow geothermal energy investigation and evaluation. 2019.
- Fang Z, Jia L, Zhang F. Heat transfer analysis of buried pipes in middle and deep layers. *J Shandong Jianzhu Univ.* 2021;36(02):1–8.
- Huang K, Luo X, Zheng Z. Modeling solute transport in karst fissure dual porosity system and application: a case study in an arsenic contamination site. *PLoS ONE.* 2020;15(6):e0234998.
- Hudson JA, Harrison JP. *Engineering rock mechanics an introduction to the principles.* 1st ed. London: Pergamon; 1997. p. 151–3.
- Jiang W, Zhou H, Li Y. Research on permeability of karst fractured media based on groundwater velocity and flow direction in boreholes. *Safety Environ Eng.* 2018;25(6):1–7+18.
- Lan Y, Tang F, Chen H. Comparative analysis of the energy-saving effect of air-conditioning system design schemes for school buildings in areas with hot summer and cold winter. *Build Energy Conserv.* 2014;42(03):4–8+14.
- Liu A, Zheng J, Li J. Comparison of evaluation methods for shallow geothermal energy and geothermal resources. *Urban Geol.* 2018;13(02):37–41.
- Lu H. Research on the evaluation and development and utilization of geothermal resources in Zhalong township, Qiqihar City. Changchun: Jilin University; 2020. p. 3–4.
- Luo J, Rohn J, Xiang W, Bertermann D, Blum P. A review of ground investigations for ground source heat pump (GSHP) systems. *Energy Build.* 2016;117(Apr):160–75.
- Ma Z, Lv Y. Design and application of ground source heat pump system. Beijing: Machinery Industry Press; 2007. p. 215.
- Ma Z, Yao Y. Civil building air conditioning design. 2nd ed. Beijing: Chemical Industry Press; 2009. p. 77.
- Mao J, Pan D, Geng S. Application research and prospect of ground source heat pump in underground engineering. *Chin J Underground Space Eng.* 2015;11(Add 1):252–6.
- Mingzhang W, Lin Z, Wei W, et al. Groundwater and geological environment in karst area of Guizhou Province. Beijing: Geological Publishing House; 2015. p. 54–8.
- Mohais R, Xu C, Dowd P. Fluid flow and heat transfer within a single horizontal fracture in an enhanced geothermal system. *Heat Transf ASME.* 2011;133(11):112603.
- Mu X, Zou H, Pei P, Lin H, Hao D. Numerical simulation research on heat exchange performance of horizontal buried heat exchanger. *Refriger Air Cond.* 2022;36(01):40–7.
- Ogino F, Yamamura M, Fukuda T. Heat transfer from hot dry rock to water flowing through a circular fracture. *Geothermics.* 1999;28(1):21–44.
- Ou Z. Guidelines for design and construction of soil source heat pump air conditioning system. Beijing: Machinery Industry Press; 2011.
- Shaik AR, Rahman SS, Tran NH, Tran T. Numerical simulation of fluid-rock coupling heat transfer in naturally fractured geothermal system. *Appl Therm Eng.* 2011;31(10):1600–6.
- Snow D. Anisotropic permeability of fractured media. *Water Resour Res.* 1969;5(6):1273–89.
- Song X, Jiang M, Peng Q, Xiong P. Analysis of thermophysical property parameters and influencing factors of main rock formations in Guizhou. *Acta Geol Sin.* 2019;93(08):2092–103.
- Sun W. Coupling simulation of groundwater seepage and ground source heat pump heat transport. *Chin J Solar Energy.* 2021;42(05):16–23.
- Wang X. Analysis and simulation of fracture characteristics of layered rock mass based on probability statistics. Beijing: China University of Geosciences; 2011.
- Wen L, Luo Z, Yang S, Wang W, Zheng K. Calculation and analysis of point load strength of rock mass damage. *J Eng Sci.* 2017;39(02):175–81.
- Xiao P, Dou B, Tian H. Numerical simulation of seepage heat transfer in single-fracture rock mass in geothermal reservoirs. *Drill Eng.* 2021;48(02):16–28.
- Xu Q, Yu Y. Correction and application of cubic law of seepage in rock fissures. *J Wuhan Univ Eng Sci.* 2022;1–9.
- Yang S, Tao W. Heat transfer. 4th ed. Beijing: Higher Education Press; 2006.
- Yang W, Zhang G, Zhang P. Hydrology and hydrogeology. Beijing: Machinery Industry Press; 2008. p. 199.
- Zhao Y, Tang L, Yu S. A review of the development of renewable energy in green buildings. *Sichuan Build Mater.* 2021;47(02):20–2+28.
- Zhou W. Selection and techno-economic analysis of hybrid ground source heat pumps used in karst landscape. *Sci Progress.* 2020a;103(2):36850420921682.
- Zhou W. Thermal accumulation risk control in the development of shallow geothermal mineral resources in karst areas. Guizhou: Guizhou University; 2020b. p. 50–1.

- Zhou H, Li J, Li T. Analysis of the hydrogeological engineering geological conditions of the Permian Qixia Maokou Formation (P₁q+m) in Huize mining area. Proceedings of the 1st yunnan youth geological science and technology forum. Kunming, China; 2017. p. 203–213.
- Zou H, Pei P, Hao D, Wang C. Numerical analysis on the effect of different soil types and moisture content on the heat transfer performance of horizontal borehole. *Coalf Geol Explor*. 2021;49(06):221–9.
- Zou H, Pei P, Zhang J. Impacts of hydrogeological characters of fractured rock on thermodynamic performance of ground-coupled heat pump. *PLoS ONE*. 2021;16(5):e0252056.
- Zou H, Pei P, Hao D, Wang C. Analysis on the Influence of Soil Hydraulic Characteristics on Heat Transfer Capacity of Horizontal Buried Pipes. *Acta Energaie Solaris Sinica*. 2022;43(5):10–20. <https://doi.org/10.19912/j.0254-0096.tynxb.2020-0905>

Publisher's Note

Springer Nature remains neutral with regard to jurisdictional claims in published maps and institutional affiliations.

Submit your manuscript to a SpringerOpen[®] journal and benefit from:

- Convenient online submission
- Rigorous peer review
- Open access: articles freely available online
- High visibility within the field
- Retaining the copyright to your article

Submit your next manuscript at ► [springeropen.com](https://www.springeropen.com)
